An Event Reconstruction Method for the Telescope Array Fluorescence Detectors

T. Fujii, M. Fukushima, K. Hayashi, K. Honda, D. Ikeda et al.

Citation: AIP Conf. Proc. **1367**, 149 (2011); doi: 10.1063/1.3628732
View online: http://dx.doi.org/10.1063/1.3628732
View Table of Contents: http://proceedings.aip.org/dbt/dbt.jsp?KEY=APCPCS&Volume=1367&Issue=1
Published by the American Institute of Physics.

An Event Reconstruction Method for the Telescope Array Fluorescence Detectors

T. Fujii[*], M. Fukushima[†], K. Hayashi[**], K. Honda[‡], D. Ikeda[†], R. Ishimori[**], Y. Kobayashi[**], S. Ogio[*], H. Sagawa[†], Y. Takahashi[†], Y. Tameda[†], H. Tokuno[**], T. Tomida[‡], Y. Tsunesada[**], S. Udo[§], K. Yamazaki[*] and the Telescope Array collaboration

[*]*Graduate Schiool of Science, Osaka City University, Sumiyoshi, Osaka 558-8585, Japan*
[†]*Institute of Cosmic Ray Research, University of Tokyo, Kashiwa, Chiba 277-8582, Japan*
[**]*Graduate School of Science and Engineering, Tokyo Institute of Technology, Meguro, Tokyo 152-8551, Japan*
[‡]*Graduate School of Medicine and Engineering, University of Yamanashi, Kofu, Yamanashi 400-8511, Japan*
[§]*Faculty of Engineering, Kanagawa University, Yokohama, Kanagawa 221-8686, Japan*

Abstract. We measure arrival directions, energies and mass composition of ultra-high energy cosmic rays with air fluorescence detector telescopes. The longitudinal profile of the cosmic ray induced extensive air shower cascade is imaged on focal plane of the telescope camera. Here, we show an event reconstruction method to obtain the primary information from data collected by the Telescope Array Fluorescence Detectors. In particular, we report on an "Inverse Monte Carlo (IMC)" method in which the reconstruction process searches for an optimum solution via repeated Monte Carlo simulations including characteristics of all detectors, atmospheric conditions, photon emission and scattering processes.

Keywords: cosmic ray, UHECR, extensive air shower, air fluorescence detector
PACS: 29.85.Fj, 95.55.Vj, 95.75.Pq

FLUORESCENCE DETECTORS OF THE TELESCOPE ARRAY EXPERIMENT

The Telescope Array (TA) experiment is an international research project designed to make precise measurements of Ultra-High Energy Cosmic Rays (UHECRs). The Telescope Array utilizes the largest air shower detector in the northern hemisphere. It consists of an array composed of 507 scintillator Surface Detectors (SDs) and 38 Fluorescence Detector (FD) telescopes. The SDs are each composed of two layers of 3 m^2 scintillator and were deployed on a 1.2 km square grid covering about 730 km^2. The FDs were deployed in three batteries on the corners of a triangle overlooking the SD array. The northern FD station, named Middle Drum (MD), has 14 telescopes which were moved from High Resolution Flys Eye (HiRes) [7] experiment. The two southern stations, named Black Rock Mesa (BRM) and Long Ridge (LR), each consist of 12 newly constructed telescopes with 3 m diameter mirrors. In all telescopes, the cameras are instrumented with 256 hexagonal PMTs, each of which views about one degree of sky.

The FD telescopes record the image of the air shower development via the UV photons emitted from atmospheric molecules excited by the air shower particles. In this paper, we report on a method of air shower reconstruction, *i.e.* to estimate an arrival direction, a primary energy and the slant depth of a maximum development point from recorded images of each shower event.

EVENT RECONSTRUCTION PROCEDURE

The data measured and recorded by the BRM and LR FDs consists of digitized waveforms of 51.2 μs length from the PhotoMultiplier Tube (PMT) for each image pixel. Figure 1 shows a sample of waveforms. The process to evaluate the information of a primary cosmic ray from data set of waveforms has three steps as follows;

1. PMT selection,
2. geometry reconstruction, and
3. shower profile reconstruction (Inverse Monte Carlo).

For each shower image we distinguish and select air shower signals for further analysis and separate them from noise signals, for example night sky background and artificial light. In geometry reconstruction, we determine the arrival direction and the core position of air showers. In shower profile reconstruction, we determine the energy and the depth of maximum development of air showers. Here, we describe an Inverse Monte Carlo" method in which we search for an optimum solution via

International Symposium on the Recent Progress of Ultra-High Energy Cosmic Ray Observation
AIP Conf. Proc. 1367, 149-152 (2011); doi: 10.1063/1.3628732

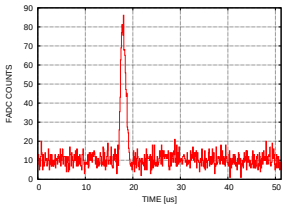

FIGURE 1. An example of recorded waveforms of PMT output. A triangle shape sign must be induced by an air shower.

repeated Monte Carlo (MC) simulations and comparing observed data with MC simulation.

PMT Selection

When fluorescence light is incident upon a PMT, the output current of the PMT is increased during $1 \sim 10\,\mu$s. The TA electronics continuously calculate the mean and the standard deviation of pedestals for the previous 1.6 ms, and tests against the trigger conditions [3]. When an event triggers the detector, 51.2μs of waveform is examined to determine the mean and standard deviation for each PMT. In order to find excess signals over the night-sky background, we calculate rolling averages in each time window of 1.6, 3.2, 6.4 and $12.8\,\mu$s. From the mean, the standard deviation and the rolling average, we calculate the maximum S/N for the waveform. Moreover, we use the triangle fitter to determine the incident timing t_i and the width σ_i of a pulse, because signal from an air shower has a triangle shape (see Figure 1). Finally, we obtained the number of photo-electrons at each PMT cathode using the calibration data [2] and pedestal information.

If signals are induced by an air shower, the fluorescence light incident upon the PMTs should clump together in a track and signal timing should be sequential. Thus, we select clumping PMTs with S/N > 6 and require that the information of isolated PMTs are removed from further analysis. Next, we examine the PMTs for sequential timing information. Additional PMT selection criteria is applied after geometry fitting and is described below.

Geometry Reconstruction

In the geometry reconstruction process, we determine the geometry of each detected air shower, *i.e.* the arrival direction and the core position.

Within our database, the directional vector for the line of sight for each PMT is stored for use in geometry reconstruction. In the analysis, the directional vector of the

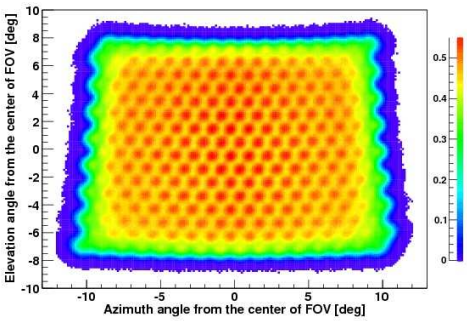

FIGURE 2. The directional characteristics of the camera (BRM camera-00).

line of sight for each PMT is defined as the weighted center angular sensitivity distribution of the triggered PMTs. From the geometrical configuration of PMTs, mirrors and telescope structures and in consideration of the non-uniformity of PMT cathode sensitivities, we evaluate angular sensitivity distributions for all the PMTs with a ray trace simulation. Figure 2 is a superimposed sensitivity map for 256 PMTs on a camera. These sensitivity maps are stored in a database and used in the analysis. The sensitivity maps are important for faster Inverse Monte Carlo calculations as we discuss later.

The geometry reconstruction begins with the determination of the shower detector plane (SDP), which is the plane with air shower axis and the position of a station. When a PMT detects fluorescence photons emitted by the air shower, the normal vector of SDP, $\vec{k}_{SDP}$ is perpendicular to the directional vector of the line of sight of the PMT $\vec{k}_i$. From a line of hit PMTs on the focal plane, an optimum solution of the normal vector of SDP minimizes $\sum_i w_i(\vec{k}_{SDP}\cdot\vec{k}_i)^2$, where w_i is the weight calculated from the number of detected photo-electrons, $w_i = n_i/\bar{n}$. n_i is the the number of photo-electrons detected on i-th PMT and $\bar{n}$ is the mean for all the hit PMTs.

Once the shower plane is determined, finding the stereo geometry reconstruction is a very simple matter by simply intersecting the two SDPs as shown in Figure 3.

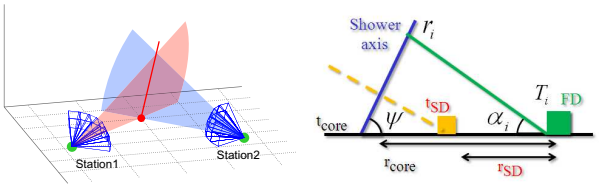

FIGURE 3. Left: stereo geometry reconstruction. Right: mono and hybrid geometry reconstruction.

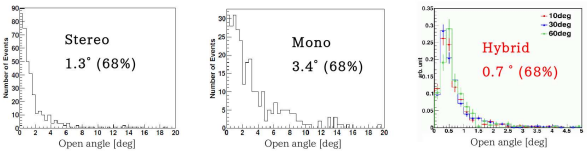

FIGURE 4. The angular resolutions in stereo, mono, and hybrid analysis.

On the other hand, in mono reconstruction (reconstruction of shower geometry with data from a single station) after determination of the SDP, the shower geometry is estimated by taking account of signal timings of each PMTs, as shown in Figure 3. In the figure, r_{core} is the core position, t_{core} is the arrival time of the shower core on the ground, ψ is the elevation angle of the shower axis direction within the SDP, and α_i is the angle between r_{core} and the projection vector of the i-th PMT's line of sight vector projected on the SDP.

We obtain the fit of the optimum geometry parameters r_{core} and ψ by minimizing the following χ^2 under the binding condition in which r_{core} is coplanar on the SDP,

$$\chi^2 = \sum_i \left[\left\{ t_i - t_{core} - \frac{1}{c} \frac{\sin\psi - \sin\alpha_i}{\sin(\psi + \alpha_i)} r_{core} \right\}^2 \Big/ \sigma_i^2 \right], \tag{1}$$

where σ_i is the arrival timing error.

The hybrid geometry reconstruction combines event data obtained from both the FDs and SDs. In this method, we add the timing information of the SD nearest to the core position for χ^2 fitting with (1) and we replace t_{core} with,

$$t_{core} = t_{SD} + \frac{1}{c}(r_{core} - r_{SD})\cos\psi, \tag{2}$$

where r_{SD} and t_{SD} are the distance from the SD to the station and the signal arrival time on the SD, respectively. Both of them are the projected values on the SDP, as shown in Figure 3.

In χ^2 fitting on mono and hybrid reconstructions, we use the timing and the position information of PMTs which have S/N > 3 and meet the selection rule of the clumpy distribution and the sequentiality.

We have evaluated resolutions of the geometry reconstruction by analyzing MC events. Figure 4 shows open angle distributions between true and reconstructed shower axis analyzed with stereo, mono and hybrid reconstructions. The 68 % confidence level is 1.3° , 3.4° and 0.7° in stereo, mono and hybrid. As shown in Figure 4, the hybrid geometry reconstruction has the best resolution.

Shower Profile Reconstruction (Inverse Monte Carlo)

The longitudinal development of an air shower can be estimated from the energy depositions along the shower axis. These are evaluated from the observed fluorescence light intensities and the shower geometry. However, this evaluation is not easy because of contamination by Čerenkov light and scattered photons, complications due to detector configurations, and non-uniformities of detector responses.

For our shower analysis we implement all the emission and scattering processes and the detector configuration into the MC code and then we use the Inverse Monte Carlo (IMC) method. In this method we search for an optimum solution while we repeatly attempting MC simulations with changing longitudinal development parameters and compare measured signals with the simulated signals for each PMT.

In this MC code we use the Gaisser-Hillas function for the longitudinal development curves. The first interaction point, X_0, and the interaction length, λ, are fixed at 0 g/cm^2 and 70 g/cm^2, respectively. The scanned values are the optimum $X_{\max}$, the slant depth of maximum development and $N_{\max}$, the shower size at $X_{\max}$.

Initially, we obtain a optimum solution of $X_{\max}$. We calculate energy deposited along the shower axis from Gaisser-Hillas function with $X_{\max}$, X_0, λ and $N_{\max} = 1.0$ and the mean ionization loss rate, $\alpha_{\rm eff}$ [4]. We use the fluorescence yield from [5] [6], Čerenkov yield from [4]. Using measured atmospheric parameters, we evaluate the number of fluorescence photons, Čerenkov photons and scattered Čerenkov photons along the shower axis. Next, we simulate signals on all the FDs with ray tracing taking into consideration the calibration constants, the atmosphere transmittance, mirror reflectivities and QE × CE [2]. In order to increase the speed of the calculations, we use a database of the sensitivity maps such as those shown in Figure 2. The number of photo-electrons $n_i^{\rm sim}$ on i-th PMT is simulated,

$$n_i^{\rm sim} = \int_x \int_\lambda N(x,\lambda) \times f_i(\vec{r}_x)\, \mathrm{d}\lambda\, \mathrm{d}x \tag{3}$$

where $N(x,\lambda)$ is the number of photons incident upon a telescope from a each slant depth x, $f_i(\vec{r}_x)$ is the sensitivity of i-th PMT. Then, we calculate the following likelihood using the observed photo-electrons $n_i^{\rm obs}$ and simulated ones $n_i^{\rm sim}$ from (3),

$$L = \sum_i \{ n_i^{\rm obs} \log \frac{n_i^{\rm sim}}{n^{\rm sim,st}} \} \tag{4}$$

$$n^{\rm sim,st} = \sum_i n_i^{\rm sim} \tag{5}$$

where $n^{\rm sim,st}$ is the total number of photo-electrons on a station from MC calculations, and $n_i/n^{\rm sim,st}$ is a proba-

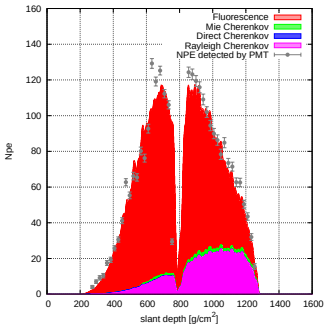

FIGURE 5. Longitudinal development curves of an observed air shower and of IMC fitting result.

bility for one photo-electron to enter the i-th PMT. While changing $X_{\rm max}$, we search for the optimum $X_{\rm max}$ with the maximum likelihood value.

After $X_{\rm max}$ is determined, we can estimate $N_{\rm max}$. Since the number of simulated photo-electrons, $n_i^{\rm sim}$, is calculated under the condition of $N_{\rm max} = 1$, we determine $N_{\rm max}$ from the ratio of the total number of detected photo-electrons to the simulated one,

$$N_{\rm max} = \frac{\sum_i n_i^{\rm obs}}{\sum_i n_i^{\rm sim}}. \qquad (6)$$

Figure 5 is an observed longitudinal development curve superimposed on the corresponding IMC fitting result. The contributions of the different emission and scattering mechanisms are shown with different colors.

The primary energy of an UHECR can be estimated from the sum of energy deposited along the shower axis. In our analysis, we first calculate the calorimetric energy, $E_{\rm cal}$, from the integration of the Gaisser-Hillas function with the optimum $X_{\rm max}$ and $N_{\rm max}$ and minimum ionization loss rate $\alpha_{\rm eff}$,

$$E_{\rm cal} = \int_{X_0}^{\infty} N_e(x, N_{\rm max}, X_{\rm max}, X_0)\,\alpha_{\rm eff}(x)\,{\rm d}x. \qquad (7)$$

Next, we correct missing energy which does not deposit in the atmosphere, such as neutral particles and their kinetic energies, and then we obtain estimate the primary energy E_0.

In order to estimate the effects of the geometrical resolution on the shower profile reconstruction, we tried to reconstruct MC events under two extreme conditions. First we use the reconstruction using the mono geometry reconstruction. next we use the true geometry. We generated MC events with energies from 10^{17} eV to 10^{20} eV and a spectral index of -3.1. As a result, the peak is low, about 10^{18} eV. Figure 6 is the histograms of reconstructed $X_{\rm max}$ and E_0 relative to thrown values, $X_{\rm max}^{\rm sim}$ and $E_0^{\rm sim}$. As shown in Figure 6, we conclude that while the

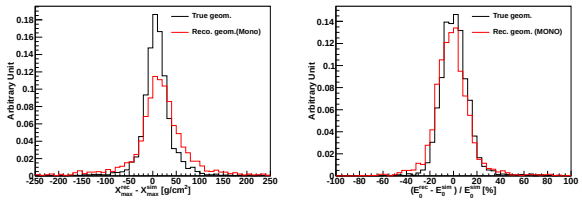

FIGURE 6. Left: the resolution of $X_{\rm max}$. Right: the resolution of E_0.

$X_{\rm max}$ resolution depends strongly on the geometry resolutions, but energy resolution is almost independent.

ACKNOWLEDGMENTS

The Telescope Array experiment is supported by the Ministry of Education, Culture, Sports, Science and Technology-Japan, Grant-in-Aid for Scientific Research on Priority Areas, "The Origin of the Highest Energy Cosmic Rays", 2003, Grant-in-Aid for Specially Promoted Research, "Extreme Phenomena in the Universe Explored by Highest Energy Cosmic Rays", 2009 and for Scientific Research (B),20340057, 2008. This experiment is also supported by the U.S. National Science Foundation (NSF) through awards PHY-0307098 and PHY-0601915 (University of Utah) and PHY-0305516 (Rutgers University). The Dr. Ezekiel R. and Edna Wattis Dumke Foundation, The Willard L. Eccles Foundation and The George S. and Dolores Dore Eccles Foundation all helped with generous donations. The State of Utah supported the project through its Economic Development Board, and the University of Utah supported us through the Office of the Vice President for Research. The use of the experimental site became possible by the cooperation of the State of Utah School and Institutional Trust Lands Administration(SITLA), the federal Bureau of Land Management(BLM) and the United States Air Force. We also wish to thank the people and the officials of Millard County, Utah, for their steadfast and warm support. We gratefully acknowledge the contributions from the technical staffs of our home institutions.

REFERENCES

1. *The Telescope Array Project Design Report* (2000)
2. H. Tokuno et al., *Nucl. Instr. and Meth. A*, 601 (2009) 364
3. Y. Tameda et al., *Nucl. Instr. and Meth. A*, 609 (2009) 227
4. F. Nerling et al., *Astropart. Phys.*, 24, 421, (2006)
5. F. Kakimoto et al., *Nucl. Instr. and Meth.* A 372, 527 (1996)
6. R. Abbasi et al., *Astropart. Phys.*, 29, 77, (2008)
7. R. Abbasi et al., *Phys. Rev. Lett.*, 100(10):101101 (2008)